Cost-Effective Bio-Synthesis and characterization of Encapsulated Cu, Ag, and Magnetic Cu-Ag Bimetallic Nanoparticles

Mahadi Hasan Shamim
University of Dhaka
Md. Faysal Kabir (faysalkabir.dup@gmail.com)
Japan Advanced Institute of Science and Technology
Jannatul Ferdousy
Green University of Bangladesh
A. K. M. Atique Ullah
Michigan State University
Rayhan Tareq
Bangladesh atomic energy commission Dhaka
Razzakul Islam
Kanazawa University
Md. Mizanur Rahman
University of Dhaka

Research Article

Keywords: Ag NPs, Cu-Ag NPs, Musa paradisiaca (Banana), synthesized, X-ray Diffraction, TGA, magnetization

Posted Date: October 27th, 2022

DOI: https://doi.org/10.21203/rs.3.rs-2172873/v1

Additional Declarations: No competing interests reported.

Version of Record: A version of this preprint was published at BioNanoScience on March 25th, 2023. See the published version at https://doi.org/10.1007/s12668-023-01083-4.

Abstract

Since this work's goal is to create magnetic monometallic and magnetic bimetallic nanoparticles will proceed without using any chemicals. This study reports the green synthesis of Cu, Ag, and Cu-Ag nanoparticles at room temperature using *Musa paradisiaca* (banana) leaf extract. Our current study also focuses on determining how effective the *leaf extract of Musa paradisiaca* (commonly known as banana) is as a reducing and stabilizing agent. After adding the *Musa paradisiaca* (banana) leaf extract to the solution containing the metal salt, constant stirring was performed until the reaction was finished. X-ray Diffraction (XRD) and the Fourier transform infrared spectroscopy (FTIR) was used to examine the synthesized nanoparticles. The major types of equipment for our characterization were Energy Dispersive X-ray Spectroscopy (EDS), Field Emission Scanning Electron Microscopy (FESEM), Thermogravimetric Analysis (TGA), and Vibrating Sample Magnetometer (VSM). The analyses revealed that *Musa paradisiaca* (Banana) leaf extract efficiently reduced the Cu, Ag, and magnetic Cu-Ag nanoparticles. Biomolecules from *Musa paradisiaca* (banana) leaves were adsorbed on nanoparticle surfaces, producing a capping layer and stabilizing the nanoparticles. The average crystalline sizes of Cu, Ag and Ag-Cu nanoparticles were about 19 nm, 13 nm, and 23.15 nm, respectively. Surface morphology and particle size distribution were also observed using a modern FESEM device. ImageJ software was used to compute the average particle size and the distribution of particle sizes. The calculated particle size range was (5nm - 35 nm), (10 nm – 60 nm), and (20 nm – 90 nm) for Cu NPS, Ag NPs, and Cu-Ag NPs, respectively. Simultaneously, the presence of elements in our synthesized nanoparticles was also investigated with the help of EDX tools. Organic functional groups were confirmed using FTIR analysis. In the last part, the magnetic behavior of our synthesis Cu-Ag bimetallic nanoparticles was analyzed using a VSM machine, and we found saturation magnetization (Ms) was 0.58 emu g^{-1}. The coercivity (Hc) was 153 Oe. According to the findings, *Musa paradisiaca* (banana) leaf extract is a promising reducing and stabilizing agent.

1. Introduction

In the last century, nanomaterials, particularly magnetic nanoparticles, have grown in research, and their applications have engrossed the focus of both scholars and industrialists [1]. Monometallic and magnetic bimetallic nanoparticles have shown promising performance in toxicity mitigation and data storage devices [2]. Magnetic nanoparticles play a role in magnetic drug targeting, which involves the application of an external magnetic field gradient to the target organ to deliver the drug by proactive targeting via ligand attachment [3]. On the other hand, it has excellent scientific concentration because of the size effect linked with its magnetic property, which is significant in nanotechnology and biomedicine [4]. When the size of the material is reduced to the nanoscale, even if it has the identical chemical make-up as bulk materials, the nanoscale may cause it to have magnetic properties that are unique from those of bulk materials [5]. The magnetic property of nanoparticles is modified by the surface electronic arrangement [6]. Numerous studies have observed that surface bindings formed with an appropriate

ligand may induce a permanent magnetism, even in nanoparticles composed of materials that are not magnetic

[7].

Because of their exceptional electrical and thermal characteristics, silver and copper nanoparticles have shown promise in a wide range of applications, which has led to significant demand for these nanoparticles in the market [8]. Reducing the size to the nanometer scale has exhibited distinct enhancements in these fundamental qualities due to the substantial surface-to-volume ratio [9]. Cu and Ag demonstrate excellent corrosion-resistant characteristics, and this resulting synthesis of their nanoparticles can be straightforwardly accomplished compared to other metals that tend to oxidize during synthesis [10]. Ag nanoparticles exhibit exclusive properties against microorganisms. Because of this, they are in great demand as ingredients in many consumer goods [11]. Moreover, these magnetic Ag nanoparticles create a new dimension in biomedicine [12]. On the other hand, Cu nanoparticles are of significant interest compared to gold, silver, and platinum for their lower cost and extensive availability [13]. Cu nanoparticles play a role in the interaction between biological reactants and catalysts for transition metal properties [14].

Some unique physicochemical and surface characteristics are developed in bimetallic nanoparticles due to the combinational interface between two metallic electronic states, poles apart from specific metals [15]. Magnetic properties in bimetallic nanoparticles and their various applications in numerous fields such as biomedical, water treatment, and sensors are the leading causes of scientific attraction [16]. Although a lot of research has been done on the preparation of monometallic nanoparticles, there are only a few reports on bimetallic nanoparticles of Cu, especially with Ag [17]. The value of the lattice constant for copper is 0.409 nm, whereas that for silver is 0.361 nm [18]. A suitable synthesis method requires synthesizing this type of large difference lattice constant bimetallic nanoparticle [19]. Various bimetallic nanoparticles, such as Cu-Ag nanoparticles, are potential candidates for linear and nonlinear optical applications [20].

The synthesis of monometallic and bimetallic nanoparticles using methods that are less harmful to the environment is the subject of many research projects that are now underway. [21]. Physio-chemical, chemical reduction, and laser ablations are very effective methods, but the risk of toxic chemicals and high operational costs are the main barriers to these methods [22]. To overcome this risk and minimize the cost, we have chosen a biogenic, cost-effective synthesis method that is environmentally safe [23]. Utilizing extracts taken from various plant parts, such as the leaves, roots, fruits, and seeds, is required to carry out this form of synthesis [24]. In the synthesis of metal and bimetallic nanoparticles, plant extracts perform the dual role of acting as reducing and stabilizing agents [25].

In this present study, we are interested in using the extract of *Musa paradisiaca* (Banana) leaves as a reducing and stabilizing agent to synthesize Cu, Ag, and Cu-Ag nanoparticles. *Musa paradisiaca* leaves are banana leaves that have substantial scientific food value. They are widely distributed worldwide with different local names. This is commonly used in therapeutic treatment. Using *Musa paradisiaca* (banana)

leaves, this is believed to be the first time that copper, silver, and magnetic copper-silver bimetallic nanoparticles have been synthesized.

2. Experimental

2.1. Materials

Musa paradisiaca (banana) leaves were collected from the University of Dhaka campus, Dhaka, Bangladesh, and $AgNO_3$ (Silver nitrate) and $Cu(NO_3)_2$ (cupper nitrate) were purchased from Wako Pure Chemical Company. The rest of the chemicals and reagents were of the highest analytical

quality.

2.2. *Musa paradisiacal* leaf extract preparation

Fresh *Musa paradisiaca* (Banana) leaves (Fig. 1) were gathered from the University of Dhaka campus, washed multiple times with water to remove dust particles, and then oven-dried at 80°C to eliminate any remaining moisture before being blinded to make a powder (Fig. 1). The plant extract was then made by combining 5 gm of plant extract with 100 ml of deionized water in a conical flask. The solution was then centrifuged for 30 minutes at room temperature at 4000 rpm. Using a vacuum filter, the supernatant was separated and filtered with **(**mm filter paper pore size**)** filter paper. After that, the solution was used to transform silver ions (Ag^{+}) into silver nanoparticles (Ag^{o}) and copper ions (Cu^{2+}) into copper nanoparticles (Cu^{0}). The leaf extract was kept at four degrees Celsius in a refrigerator at the Atomic Energy Center in Dhaka. In Fig. 1, which is the schematic diagram of our current study, all of the processes of our following synthesis are presented.

2.3. Copper (Cu), Silver (Ag), and Copper-Silver (Cu-Ag) nanoparticles synthesis

To 150 ml of leaf extracts, 300 mL of a combination solution consisting of 50 mM [$AgN0_3$ and $Cu(NO_3)_2$] was added at a ratio of 1:1. (supernatant). After that, the solution was vigorously shaken by hand to guarantee that it was completely combined. After that, a magnetic string was used to agitate the solution at 70 degrees Celsius for one hour. In order to produce Cu-Ag bimetallic nanoparticles, the reaction was allowed to finish off at room temperature. Synthesizing silver and copper nanoparticles required a process that was quite similar, and it was carried out using solutions of $AgNO_3$ and $Cu(NO_3)_2$. The process was carried out quite a few times.

2.4. Characterization techniques

In the powder form, the X-ray diffraction patterns of copper (Cu), silver (Ag), and copper-silver (Cu-Ag) bimetallic nanoparticles were investigated. The powder samples were compacted in a square aluminum sample container (40 mm × 40 mm) with a one-millimeter-deep rectangular hole (20 mm × 15 mm) and

pushed against an optically smooth glass panel. In the same plane as the top surface of the sample, the sample holder's label was affixed to the plane. Following that step, the sample holder was installed into the diffractometer. EDS spectra were used to carry out elemental analysis on the silver, copper, and Cu-Ag nanoparticles that were artificially produced. The dried powders of nanoparticles were put on a conductive steel plate of 1 centimeter by 1 centimeter. After that, the steel plate was positioned above a conductive carbon strip that had been bonded. The sample was transferred into the main chamber of the SEM, which also included the EDS equipment. The use of scanning electron microscopy was used in order to determine the surface morphology of the nanoparticles. On a strip of conducting carbon that had been bonded together, the dried powders that had been manufactured were disseminated. After the sample-loaded strip was affixed to a chamber, the chamber was evacuated to a pressure of 10^{-3} to 10^{-4} torr. A very thin coating of gold was sputtered on the sample to guarantee that the sample surface had enough conductivity. After that, the sample was transferred to the primary SEM chamber to examine its surface. Because the system could communicate with computers, it was able to save a recording of the surface pictures in a computer file, which could then be printed out as a tangible copy. In order to compute the particle size and distribution, the program known as "ImageJ" was used. An FTIR spectrometer was used to record infrared spectra in the range of 4000–400 cm-1 for dried samples of banana leaf powder as well as synthesized Copper(Cu), Silver(Ag), and Copper-Silver(Cu-Ag) bimetallic nanoparticles. These spectra were taken in the infrared spectrum region known as the Fourier transform infrared. Mixing and grinding a limited number of materials with dry and pure KBr crystals often resulted in the production of IR spectra of the solid samples. In a mortar, a pestle was used to crush and mix the ingredients. The powder combination was placed in a metal container and subjected to between 8 and 10 tons of pressure to create a pellet.

After that, the pellet was positioned such that it would be illuminated by the IR beam so that measurements could be taken. In a muffle furnace, the silver nanoparticles were subjected to heat treatment for three hours at temperatures of 100°C, 200°C, 300°C, 400°C, 500°C, 600°C, 700°C, and 800°C. This was done so that the influence of temperature on phase change could be investigated. Experiments using a VSM (German: EV-9 Micro Sense) were carried out in the last step to evaluate the magnetic behavior of the Cu-Ag bimetallic nanoparticle that we had just manufactured. During this inquiry, the first thing that needed to be done was to construct a vibrating mechanism capable of vibrating the sample at an amplitude that was both measurable and adjustable. The last phase consisted of a magnetic field employed to cause disturbances, and the detecting coils were used to measure it.

3. Results And Discussion

3.1. X-Ray Diffraction (XRD) analysis

XRD is the most effective and famous technique to measure crystal structure and crystalline size, which means it can give comprehensive information about crystal structure. The crystalline nature of the Cu NPs has been confirmed as the biosynthesized technique by XRD and the representative XRD patterns,

which are shown in Fig. 2 (a). The diffraction peaks were obtained at the 2θ values corresponding to the planes (110), (111), and (200), which were 36.38^0, 43.36^0, and 50.35^0 respectively. This XRD result suggests that the prepared Cu NPs are face-centered cubic [26]. The average crystallite size of the prepared samples was determined from the most substantial peak using Scherrer's formula, and the calculated crystallite size was about 19 nm.

XRD confirmed Ag NPs and Cu-Ag NPs as crystalline in the biosynthesized technique, and the representative patterns are shown in Fig. 2 (b). The diffraction peaks (Ag NPs) were obtained at the 2θ values corresponding to the plane (110), (111), (200), and (220) were 38.20^0, $44.45^{0,}$ and $64.41^{0,}$ respectively. This result also recommends that the prepared Ag NPs be face-centered cubic [27]. Moreover. The average crystallite size was calculated from the most substantial peak using Scherrer's formula, and the considered crystallite size was about 13 nm. Similarly, (Cu-Ag NPS) 2θ values corresponding to the planes (110), (111), (200), and (220) are 38.19^0, 44.42, and 64.61^0, respectively. Compared with the standard curve, our prepared Cu-Ag NPs are face-centered cubic in nature [28]. Here we see that Ag is the dominating part of Cu-Ag nanoparticles, and the XRD peaks are associated with silver nanoparticles, which are found in Fig. 2 (b). The average crystallite size of the prepared samples was determined from the most substantial peak, and the calculated crystallite size was about 23.15 nm. In the above three XRD patterns, some unsigned peaks may be associated with the organic compounds that originate from the banana leaf extract and act as capping agents. These unsigned peaks also support the FTIR data, where we found many organic compounds.

3.2. Energy Dispersive X-ray (EDS) spectroscopy analysis

Elemental analysis of the synthesized bio-organic components coming from *Musa paradisiaca* leaf extract was performed using EDS spectra analysis and is shown in Fig. 3. (a) Cu NPs, (b) Ag NPs, and (c) Cu-Ag NPs. This is very clear in Fig. 3. (a), The EDS profile has shown strong signals for silver atoms. The strong signal peak at 7.8 keV in the EDS spectrum was typical of the absorption of silver nanocrystallites [29], and the weak signals are found at 1 keV, 8.5 keV, and 9.0 keV, which establishes the presence of Ag NPs.

In Fig. 3. (b), the EDS profile showed solid signals for copper atoms. The strong signal peak at 0.9 keV in the EDS spectrum was typical of the absorption of copper nanocrystallites, and the weak signal peak at 8 keV and 9 keV was also found.

Further investigation of bimetallic nanoparticles, the EDS profile Fig. 3. (c) provided strong signals for copper and silver atoms. The strong signal peak at 0.9 keV in the EDS spectrum was distinctive from the absorption of copper nanocrystals. The weak signals were in 0.3 keV, 0.7 keV, 8.0 keV, and 9.0 keV strongly exhibited the presence of copper nanoparticles [30]. The strong signal peak at 3.0 keV in the EDS spectrum was typical of the absorption of silver nanocrystallites, and the weak signals at 3.2 keV and 3.5 keV strongly showed the presence of silver nanoparticles [31]. So, this showed the presence of Cu-Ag NPs.

In the above three EDS spectra, some other elements, interestingly details features such as C, N, and O, were also detected. C, N, Cl, and O are likely associated with the organic compounds from the banana leaf extract absorbed on the surface of Cu NPs, Ag NPs, and Cu-Ag NPs, which play a crucial role in the reduction and stability. Even if we carefully observe the XRD pattern's unsigned peak, which supports these extra elements in the EDS signal, most of which are organic compounds. Moreover, this organic compound is mainly responsible for reducing and stabilizing the nanoparticles [30–31].

3.3. Field Emission Scanning Electron Microscopy (FESEM) analysis

The surface morphology of the synthesized nanoparticles was monitored using Field Emission Scanning Electron Microscopy (FESEM) technique and shown in Fig. 4. The FESEM image of 4 (a) Cu NPs, (b) Ag NPs, and (c) Cu-Ag NPs clearly showed that the green synthesized nanoparticles were uniformly distributed with lowering agglomeration. The gross calculation can be drawn from the image of part of the size range. It was evident in the SEM image that all of the particles were in the nao scale range. We used the popular software named "ImageJ" for more accurate calculation. After analyzing the result, the particle size range for (a) Cu NPs, was found (5nm – 35 nm). Maximum particle distribution belongs to (12 nm-18 nm), and the average particle size is about (17 nm), which is enough for nanoparticle confirmation. In Fig. 4 (b) for Ag NPs, most of the particles were in a nanoscale range which can define as (10 nm – 60 nm). Most of the particle Particles were distributed from 15 nm to 30 nm. The number of particles in the lower and upper range was not huge. The average particle size was calculated at about 24 nm, slightly greater than Cu NPs. Cu-Ag bimetallic nanoparticles' size value started from 20 nm, and the maximum range of particles was about 90. In the region, 40 nm -50 nm ultimate particles were obtained, and the average size of the whole particles was 48 nm. The average size is slightly larger than previous Cu NPs and Ag NP's average size. At the calculation time, few particles in the above three types were larger than intermediate particles. The large particles were probably due to the accumulation of small ones [32]. The large particle may be reduced by heat treatment. Identical results were also found in different experiments where agglomeration is mainly responsible for obtaining large particles [33]. The lowering of the aggregation might be due to the presence of capping agents on the surface of Ag NPs, Cu NPs, and Cu-Ag NPs, which was also evidenced by the EDX and FT-IR analyses.

3.4. Fourier Transform Infrared (FT-IR) spectra analysis

Cu NPs (a) are shown in Fig. 5, and the resulting peaks correspond to the following frequencies: 482.20 cm^{-1}, 1099.43 cm^{-1}, 1365.60 cm^{-1}, 1624.06 cm^{-1}, 3435.22 cm-1, and 3772.76 cm^{-1}. Table 1 contains a tabulation of those peaks arranged according to the functional category they belong to. Numerous additional bioorganic compounds can exist in the solution and contribute to reducing copper ions and stabilizing the nanoparticles generated due to surface capping. At this time, we were working on isolating the various bioorganic fractions in the banana leaf broth so that we may examine each one separately for its ability to inhibit copper ion reduction and to bond with nanoparticles.

Table 1

Summary of (FT-IR) spectra analysis of Banana leaf, Banana leaf extract mediated (a) Cu NPs, (b) Ag NPs, (c) Cu-Ag NPs, and (d) *Musa paradisiaca* leaf (Banana leaf) powder

Spectrum number and name	Wave number	Functional group	Reference
(a) Cu NPs	i).482.20cm^{-1} ii).1099.43cm^{-1} iii). 1365.60cm^{-1} iv). 1624.06cm^{-1} v). 3435.22 cm^{-1} vi). 3772.76 cm^{-1}	i). (Alkyl Halide) ii). (Alcohol) or C-N (Amine) iii). C-H for (Alkane) or C-F (Alkyl Halide) iv). C=C(Alkene) v). O-H (Alcohol) vi). N-H (Amine)	[34]
(b) Ag NPs	i) 470.63cm^{-1} ii) 1083.99cm^{-1} iii) 1355.96cm^{-1} iv) 1602.85cm^{-1} v) 3435.22cm^{-1}	i) (Alkyl Halide) ii)(Alcohol)/C-N (Amine) iii) C-H for (Alkane) or C-F (Alkyl Halide) iv) C=C(Alkene) v) (Alcohol) or N-H (Amine)	[35]
(c) Cu-Ag NPs	i) 478.35cm^{-1} ii) 1060.85cm^{-1} iii) 1379.10cm^{-1} iv) 1622.13cm^{-1} v)3437.15, 3693.68, 3770.84 cm^{-1}	i) (Alkyl Halide) ii)(Alcohol)/C-N (Amine) iii) C-H for (Alkane) or C-F (Alkyl Halide) iv) C=C(Alkene) v) (Alcohol) or N-H (Amine)	[36,37]
(d) *Musa paradisiaca* **leaf (Banana leaf) powder**	i) 518.85cm^{-1} ii) 653.87cm^{-1} iii) 1066.64 cm^{-1} iv)1321.24cm^{-1}, 1384.89cm^{-1} v) 1629.85cm^{-1}	i) (Alkyl Halide) ii)C-Cl (Alkyl chloride), iii) O-H (Alcohol) or C-F (Alkyl fluoride), iv) different types of amine group (N-H), v) C=C (Alkene) or C=O (Carbonyl), vi) alkanes C-H vii) N-H (Amine) viii) O-H (Alcohol)	[37]

vi) 2860.43cm^{-1}, and 2922.16cm^{-1}

vii) 3429.43cm^{-1}

viii) 3711.04 cm^{-1}, and 3770.84 cm^{-1}

In Fig. 5, the locations of the peaks at 470.63 cm^{-1}, 1083.99 cm^{-1}, 1355.96 cm^{-1}, 1602.85 cm^{-1}, and 3435.22 cm^{-1} were revealed in the curve "b" which was the FTIR spectrum of the produced Ag NPs. It was compared to common values, and a few organic groups were also discovered for the location of the peaks above it. In the end, each and every one of them was included in Table 1. Terpenoids were also responsible for the reduction of silver ions. During this process, the terpenoids were oxidized to carbonyl groups, which led to the formation of a band at 1602.85 cm^{-1}. The peak corresponding to the amine band at 1083.99cm^{-1} has enlarged due to the creation of Ag NPs, which shows that the protein is responsible for capping the silver nanoparticles [34]. It is well known that proteins may attach to silver nanoparticles (Ag NPs) through free amine group residues [35]. It has been shown that plants exude many secondary metabolites that encompass a wide variety of organic structures. A variety of additional bioorganic substances were capable of being in the solution and taking part in lowering the number of silver ions while simultaneously stabilizing the nanoparticles.

Represented the leaf extract mediated (curve “c”) Cu-Ag NPs, and the peaks that were produced corresponded to the following wavelengths: 478.35cm^{-1} for (Alkyl Halide), 1060.85cm^{-1} for (Alcohol) or C-N (Amine), 1379.10cm^{-1} for C-H for (Alkane) or C-F (Alkyl Halide), 1622.13cm The peak that corresponds to the amine band at 1060.85cm^{-1} has expanded during the creation of Ag NPs, which shows that the protein is responsible for capping the copper and silver nanoparticles [36]. It is also well knowledge that proteins include free amine group residues that, when exposed to Cu-Ag NPs, may cause a binding reaction [37].

An FT-IR spectrometer recorded the spectra of Fourier Transform Infrared (FT-IR) on a dried sample of *Musa paradisiaca* (Banana) in the area of wavenumber ranging from 4000 to 400 cm^{-1} vs. transmittance varying from 60–100 percent. These results are shown in Fig. 5. (curve “d”). The corresponding organic functional groups for peak values were maybe 518.85 cm^{-1} for C-X (alkyl halide), 653.87 cm^{-1} for C-Cl (Alkyl chloride), 1066.64 cm^{-1} for O-H (alcohol) or C-F (alkyl fluoride), 1321.24 cm^{-1}, 1384.89 cm^{-1} for various types of an amine group (N-H), and 1629.85 cm^{-1} for The simple *Musa paradisiaca* leaf, sometimes known as the banana leaf, had no harmful functional groups in any of its constituent components. The results of the four spectra were summarized in Table 1.

The leaf extract solution was most likely the origin of the bioorganic component that was used in the synthesis of copper nanoparticles, silver nanoparticles, and copper-silver nanoparticles (Cu-Ag NPs). Therefore, it is possible to hypothesize that numerous bioorganic composites are present in the solution

and contribute to the reduction of copper and silver ions and the stability of the nanoparticles generated as a result of surface capping. The *Musa paradisiaca* leaf, sometimes known as banana leaf, served as the basis for this non-hazardous and effective pesticide alternative.

3.5. Thermo Gravimetric Analysis (TGA)

To examine the thermal stability of (a) Cu NPs, (b) Cu-Ag NPs, and (c) Ag NPs in (Fig. 6), Thermo Gravimetric Analysis (TGA) was carried out between 24^0C and 800°C and the corresponding data was shown in Fig. 6. The weight loss in the first 13.23 min was observed up to 166.08°C (4.03%) (Fig,6, curve a), which may be attributed to the release of water molecules adsorbed on the surface of Cu NPs. The weight loss for 54.41 min was obtained up to 577.38°C (36.10%), which might be due to the release of organic compounds attached to the surface of Cu NPs acting as capping agents.

To study the thermal stability of bimetallic Cu-Ag NPs, Thermo Gravimetric Analysis (TGA) was carried out. The weight loss in the first 15.80 min was observed up to 181.44°C (4.6%) (Fig. 6, curve b), which may be associated with the release of water molecules on the surface Cu-Ag NPs. The weight loss in a time of 57.54 min was detected at 600.98°C (25.32%) mainly occurred to releasing organic compounds attached to the surface of Cu-Ag NPs. The weight loss by increasing temperature is less than Cu and Ag nanoparticles.

Similarly, in the case of Ag NPs, the weight loss in the first 19.32 min was observed up to 220.09°C (6.77%) (Fig. 6, curve c) for releasing water molecules from the surface of Ag NPs. The weight loss in 54.33 min was found up to 570.64°C (38.99%), which might be due to the release of attached organic compounds on the surface of Ag NPs acting as capping stabilizing agents. Similar studies were reported by earlier workers [38]. The EDS and FT-IR analyses also evidenced the presence of capping and stabilizing agents.

3.6. Magnetic property analysis

The magnetic property of synthesized Cu-Ag NPs was examined using Vibrating Sample Magnetometer (VSM) analysis, and the corresponding hysteresis loop was shown in Fig. 7. The hysteresis loops of the VSM analysis showed that the synthesized Cu-Ag NPs showed a ferromagnetic nature at room temperature. The saturation magnetization (M_s) was calculated as 0.58 emu $g^{-1,}$ and the coercivity (H_c) was 153 Oe.

It is common knowledge that the size of nanomaterials plays a significant part in determining their electrical, chemical, optical, and magnetic characteristics. The discovery that nanoparticles of materials like metal oxides and other inorganic materials may exhibit ferromagnetism, even though the bulk state of these substances is diamagnetic [39]. The charge transfer generated by the 5d localized holes in this

nanoparticle gives it its ferromagnetic property [40]. Since the charge is being transferred, the formation of orbital magnetism from spin-orbit couplings has been a topic of discussion [41]. Researchers believe that the ferromagnetic character of surface Nobel atoms, caused by the Fermi hole effect, is responsible for the dependency of ferromagnetism on particle size. An X-ray circular dichroism investigation concluded that nanoparticle spin polarization is due to localized holes [41]. According to a number of the findings, it would seem that the presence of thiol or amine capping agents is required for the magnetism of nanoparticles. The ferromagnetic behavior of our green synthesized Cu-Ag NPs could be said to be due to the Nano-sized dimension and the presence of amine or thiol groups on the surface of Cu-Ag NPs, which also agreed well with the EDX and FT-IR analyses. In our earlier studies, we demonstrated that produced silver nanoparticles had magnetic properties [24]. According to the findings of this work, it was also weakly ferromagnetic in bimetallic forms such as Cu-Ag nanoparticles. In addition, most of the bimetallic that we synthesized consisted of silver.

4. Probable Biological Application Of Our Synthesized Nps

4.1. Bio-application of Ag NPs:

The particularly notable focus was placed on the biomedicine-related evaluation of Ag NPs, which drew first global interest as unconventional antibacterial agents [42]. Ag NPs have been employed as antibacterial agents in the medical field for a very long period, despite the fact that there is little information available on their toxicity and in vivo biological behaviour [42]. Ag NPs have been extensively studied in addition to their inherent antibacterial uses because of their advantageous size-related physicochemical properties shown in new electronic, magnetic, catalytic, and optical materials [43]. Because of its numerous characterization parallels to earlier Ag NPs-related research that has been successful in biological applications, the literature study confirms that our synthesized Ag Nanoparticles may be a prospective contender for the health business. Since Ag NPs instability in bacterially rich settings and loss of their anti-pathogenic action pose a specific restriction to their application as antimicrobials, enhancing their stability is of special interest [43]. Numerous synthetic, natural, biotic, and antibiotic compounds have been utilized as capping agents to increase the stability of Ag NPs in the solution [44]. As an automated reducing and capping agent, plant leaf extract was used in our investigation to manufacture Ag NPs. Additionally, all of the extract's components were completely non-toxic and eco-friendly, which are important requirements for use in medicine.

The following phenomena are likely how our synthesized Ag NPs would exert their antibacterial properties, according to a literature analysis: (a) Damage to bacterial membranes brought on by the physically and chemically guided attachment of Ag NPs to the cell surface and the ensuing structural and functional changes, and (b) damage to bacterial sub-cellular structures brought on by the release of free Ag^+ ions and the subsequent generation of reactive oxygen species (ROS) or the inactivation of crucial macromolecules (proteins, enzymes, and nucleotides) [45]. Ag NP-based antimicrobial effects adhesion to microbial cells, production of ROS and free radicals, microbial wall piercing and penetration inside cells, and modulation and modification of microbial signal-transduction pathways, however, represent

their most striking mechanistic mode of action [45]. The shape, size, oxidation and dissolution states, surface charge, and surface coating of our produced Ag NPs may all have a significant impact on their biological activity [44, 45]. We have high expectations that our bio-synthesized Ag NPs will be utilized to create novel, performance-improving Nano silver-based biomedical goods such anticancer agents, drug delivery systems, orthopaedic materials and devices, bandages, antiseptic sprays, and catheters. A thorough understanding of the related physicochemical particularities, in vitro and in vivo effects, and safety control mechanisms of our synthesized non-toxic Ag NPs is also necessary for their use in clinical applications [46]. These methods must be safe, straightforward, environmentally friendly, and cost-effective.

4.2. Bio-application of Cu NPs:

All living things have a metabolism, and fermentation is where copper is predominantly found [47]. In investigations using Escherichia coli, other nanoparticles, such as platinum, gold, iron oxide, silicon oxides, and nickel, did not exhibit bactericidal effects [48]. Cu demonstrated an advantage over Ag in the antibacterial investigation utilizing Cu NPs and Ag NPs on *E. coli* and *Bacillus subtilis* [49]. Furthermore, copper and its derivative have been used as antiviral and antifungal drugs [49]. It is crucial to create a green approach for producing Cu NPs that is safe, dependable, affordable, biocompatible, and non-toxic. Due to the existence of several bioactive chemicals in plants, numerous plant parts or whole plants have been employed for the green production of Cu NPs. Jackfruit leaf was used in our study as a reducing and capping agent. As a result, the whole substance is harmless since there have never been any reports of harmful substances being present in jack fruit leaves. On the other hand, jackfruit leaf extract contains a variety of beneficial components that may be quite helpful in both biological applications and medicinal treatment [50]. According to the previous literature study, Cu NPs had a strong fungicidal effect on *Penicillium spp*. microorganisms and a positive antibacterial effect on *Bacillus spp.* Cu NPs were furthermore used for their cytotoxic and antioxidant properties [49, 50].

4.3. Bio-application of bimetallic Cu-Ag NPs:

Numerous studies have been conducted on bimetallic nanoparticles (NPs) made of copper (Cu) and silver (Ag) that have a high surface atom content and a sizable specific surface area [51]. Individually, metals like Cu and Ag do not have interesting optical, catalytic, or structural capabilities. On the other hand, fusing the two metals (Cu-Ag) opens up additional possibilities for adjusting the final product's shape and structure. A research team found that the binding interaction pattern of these NPs within the active pocket was revealed by molecular docking analysis of Cu-Ag NPs against enzyme targets of the cell wall along with the fatty acid biosynthesis pathway [51]. The enzyme targets were chosen from *A. bauminnii*, *S. aureus*, and *E. coli* keeping in mind these microorganisms' in vitro antibacterial capability for these NPs in order to obtain insight into the putative mechanism behind their bactericidal action. Ag-Cu BNPs were originally tested for their antibacterial efficacy against *Ps. syringae*, *P. carotovorum*, and *E. amylovora*, three Gram-negative plant pathogenic bacteria [52]. Comparing the MNPs to the Ag-Cu BNPs, the activity was much greater. The composites have shown substantial action against all three of the studied pathogens even at a low dose (1 mg/l) [52]. With regard to all three diseases, the Cu-Ag nanocomposites

that were created in an alkaline solution showed the greatest activity. Because they share many traits with previously produced Cu-Ag bimetallic nanocomposites that had a significant impact on biological applications, our Cu-Ag nanocomposites have also emerged as prospective candidates in this field.

5. Conclusion

Through the reduction process with the leaves of *Musa paradisiaca* (banana), it was possible to effectively produce copper (Cu), silver (Ag), and magnetic copper-silver (Cu-Ag) bimetallic nanoparticles. The average crystalline size of Cu nanoparticles was 19 nm, whereas that of Ag nanoparticles was 13 nm, and that of Cu-Ag nanoparticles was 23.15 nm. In every SEM investigation, the particle range was found to be below 100 nm. Experiments using FTIR and EDS indicated that the organic chemicals found in leaf extract acted as capping and reducing agents. The magnetic properties were seen in the produced bimetallic Cu-Ag nanoparticles. The discovery of the creation of magnetic bimetallic Cu-Ag nanoparticles by the green synthesis approach, which was weakly ferromagnetic, was this study's original and innovative contribution. Because there has been no prior investigation into the magnetic properties of biosynthesized Cu-Ag bimetallic NPs, this is an intriguing and innovative new line of inquiry. The influence of magnetic characteristics has the potential to become a fruitful area of study in the future.

Declarations

Acknowledgement

The authors would like to acknowledge Materials Science Division, Atomic Energy Centre Dhaka; Department of Physics, University of Dhaka; and Department of Glass and Ceramic Engineering, Bangladesh University of Engineering and Technology for their assistance for the characterization; School of Material Science, Japan Advanced Institute of Science and Technology (JAIST) and Kanazawa University for their cooperation

Funding: This research did not receive any specific grant from funding agencies in the public, commercial, or not-for-profit sector.

Conflict of Interest: The authors declare that they have no conflict of interest.

Ethical approval: This article does not contain any studies with human participants or animals performed by any of the authors

Authors contribution: *Mahadi Hasan Shamim and Md. Faysal Kabir have equally contributed to this article. All authors contributed to the study conception and design. Material preparation, data collection and analysis were performed by [Mahadi Hasan Shamim], [Md. Faysal Kabir], [Jannatul Ferdousy], [A.K.M. Atique Ullah] and [Md. Mizanur Rahman]. All the figures were drawn in origin by [Rayhan Tareq], [Razzakul Islam] and [Jannatul Ferdousy]. The first draft of the manuscript was written by [Md. Faysal*

Kabir] and all authors commented on previous versions of the manuscript. All authors read and approved the final manuscript.

Availability of data and Materials: Not applicable

References

1. Gholami-Shabani M, Gholami-Shabani Z, Shams-Ghahfarokhi M., Jamzivar F, Razzaghi-Abyaneh M (2017) Green nanotechnology: biomimetic synthesis of metal nanoparticles using plants and their application in agriculture and forestry. In Nanotechnology 20: 133-175. https://doi.org/10.1007/978-981-10-4573-8_8
2. Modisha PM, Ouma CN, Garidzirai R, Wasserscheid P, Bessarabov D (2019) The prospect of hydrogen storage using liquid organic hydrogen carriers. Energy & fuels 33: 2778-2796. https://doi.org/10.1016/j.commatsci.2019.109332
3. Calzoni E, Cesaretti A, Polchi A, Di Michele A, Tancini B, Emiliani C (2019) Biocompatible polymer nanoparticles for drug delivery applications in cancer and neurodegenerative disorder therapies. Journal of functional biomaterials 10: 4-10. https://doi.org/10.3390/jfb10010004
4. Cardoso VF, Francesko A, Ribeiro C, Bañobre-López M, Martins P, Lanceros-Mendez S (2018) Advances in magnetic nanoparticles for biomedical applications. Advanced healthcare materials 7: 1700845-1700853. https://doi.org/10.1016/j.cej.2018.09.173
5. Ruso JM, Hassan N (2018) Role of Biomacro molecules in Biomedical Engineering. Current TopicsinMedicinalChemistry 18:11711187. http://dx.doi.org/10.2174/1568026618666180816155917
6. Guo Y, Xu K, Wu C, Zhao J, Xie Y (2015) Surface chemical-modification for engineering the intrinsic physical properties of inorganic two-dimensional nanomaterials. Chemical Society Reviews 44: 637-646. https://doi.org/ 10.1039/c4cs00302k
7. Bohara RA, Thorat ND, Pawar SH (2016) Role of functionalization: strategies to explore potential nano-bio applications of magnetic nanoparticles. RSC advances 6: 43989-44012. https://doi.org/10.1039/C6RA02129H
8. Bhanushali S, Ghosh P, Ganesh A, Cheng W (2015) 1D copper nanostructures: progress, challenges and opportunities. Small 11: 1232-1252. https://doi.org/10.1002/smll.201402295
9. Khan I, Saeed K, Khan I (2019) Nanoparticles: Properties, applications and toxicities. Arabian journal of chemistry 12: 908-931. https://doi.org/10.1016/j.arabjc.2017.05.011
10. Gawande MB, Goswami A, Felpin FX, Asefa, T, Huang X, Silva R, Zou X, Zboril R, Varma RS (2016) Cu and Cu-based nanoparticles: synthesis and applications in catalysis. Chemical reviews 116: 3722-3811.https://doi.org/10.1021/acs.chemrev.5b00482
11. Keat, CL, Aziz A, Eid AM, Elmarzugi NA (2015) Biosynthesis of nanoparticles and silver nanoparticles. Bioresources and Bioprocessing 2: 1-11. https://doi.org/10.1186/s40643-015-0076-2

12. Arias LS, Pessan, JP, Vieira APM, Lima TMTD, Delbem ACB, Monteiro DR (2018) Iron oxide nanoparticles for biomedical applications: a perspective on synthesis, drugs, antimicrobial activity, and toxicity. Antibiotics 7: 46-54. https://doi.org/10.3390/antibiotics7020046
13. Amiripour F, Azizi SN, Ghasemi S (2018) Gold-copper bimetallic nanoparticles supported on nano P zeolite modified carbon paste electrode as an efficient electro catalyst and sensitive sensor for determination of hydrazine. Biosensors and bioelectronics, 107: 111-117. https://doi.org/10.1016/j.bios.2018.02.016
14. Li Z, Yu L, Milligan C, Ma T, Zhou L, Cui Y, Qi Z, Libretto N, Xu B, Luo J, Shi E (2018) Two-dimensional transition metal carbides as supports for tuning the chemistry of catalytic nanoparticles. Nature communications, 9: 1-8. https://doi.org/10.1038/s41467-018-07502-5
15. Singla R, Guliani A, Kumari A, Yadav SK (2016) Metallic nanoparticles, toxicity issues and applications in medicine. In Nanoscale materials in targeted drug delivery, theragnosis and tissue regeneration 87: 41-80. https://doi.org/10.1007/978-981-10-0818-4_3
16. Sharma G, Kumar A, Sharma S, Naushad M, Dwivedi RP, ALOthman ZA, Mola GT (2019) Novel development of nanoparticles to bimetallic nanoparticles and their composites: a review. Journal of King Saud University-Science 31: 257-269.https://doi.org/10.1016/j.jksus.2017.10.002
17. Sharma G, Kumar D, Kumar A, Ala'a H, Pathania D, Naushad M, Mola GT (2017) Revolution from monometallic to tri metallic nanoparticle composites, various synthesis methods and their applications: a review. Materials Science and Engineering 71: 1216-1230. https://doi.org/10.1016/j.msec.2016.11.002
18. Wu W, Lei M, Yang S, Zhou L, Liu L, Xiao X, Jiang C, Roy VA (2015) A one-pot route to the synthesis of alloyed Cu/Ag bimetallic nanoparticles with different mass ratios for catalytic reduction of 4-nitrophenol. Journal of Materials Chemistry 3: 3450-3455. https://doi.org/10.1186/s11671-019-2862-9
19. Daniel YS, Aziz ZA, Ismail Z, Salah F (2017) Numerical study of entropy analysis for electrical unsteady natural magneto hydrodynamic flow of nanofluid and heat transfer. Chinese Journal of Physics 55: 1821-1848. https://doi.org/10.1016/j.jksus.2017.10.002
20. Sharma V, Maivizhikannan V, Rao VN, Kumar S, Kumar A, Kumar A, Shankar MV, Krishnan V (2021) Sea urchin shaped ZnO coupled with MoS2 and polyaniline as highly efficient photo catalysts for organic pollutant decomposition and hydrogen evolution. Ceramics International 47: 10301-10313. https://doi.org/10.1016/j.ceramint.2020.09.199
21. Martina K, Manzoli M, Gaudino EC, Cravotto G (2017) Eco-friendly physical activation methods for Suzuki–Miyaura reactions. Catalysts 7: 98-107. http://dx.doi.org/10.3390/molecules23102435
22. Akter M, Sikder MT, Rahman MM, Ullah AA, Hossain KFB Banik S, Hosokawa T, Saito T, Kurasaki M (2018) A systematic review on silver nanoparticles-induced cytotoxicity: Physicochemical properties and perspectives. Journal of advanced research 9: 1-16. https://doi.org/10.1016/j.jare.2017.10.008
23. EL Moslamy (2018) Bioprocessing strategies for cost-effective large-scale biogenic synthesis of nano-MgO from endophytic Streptomyces coelicolor strain E72 as an anti-multidrug-resistant

pathogens agent. Scientific reports 8: 1-22. https://doi.org/10.1166/nnl.2019.2901

24. Ullah AMA, Kabir MF, Akter M, Tamanna, AN, Hossain A, Tareq ARM, Khan MNI, Kibri AF, Kurasaki M, Rahman MM (2018) Green synthesis of bio-molecule encapsulated magnetic silver nanoparticles and their antibacterial activity. RSC advances 8: 37176-37183. https://doi.org/10.1039/C8RA06908E
25. Kuppusamy, P, Yusoff, MM, Maniam GP, Govindan N (2016) Biosynthesis of metallic nanoparticles using plant derivatives and their new avenues in pharmacological applications–An updated report. Saudi Pharmaceutical Journal 24: 473-484. https://doi.org/10.1016/j.jsps.2014.11.013
26. Manoj D, Saravanan R., Santhanalakshmi J, Agarwal S, Gupta VK, Boukherroub R (2018) Towards green synthesis of monodisperse Cu nanoparticles: an efficient and highly sensitive electrochemical nitrite sensor. Sensors and Actuators 266: 873-882 https://doi.org/10.1016/j.snb.2018.03.141
27. Soto KM, Quezada-Cervantes CT, Hernández-Iturriaga M, Luna-Bárcenas G, Vazquez-Duhalt R, Mendoza S (2019) Fruit peels waste for the green synthesis of silver nanoparticles with antimicrobial activity against foodborne pathogens. Lwt 103: 293-300, https://doi.org/10.1016/j.lwt.2019.01.023
28. Ashishie PB, Anyama CA, Ayi AA, Oseghale CO, Adesuji ET, Labulo AH (2018) Green synthesis of silver monometallic and copper-silver bimetallic nanoparticles using Kigeliaafricana fruit extract and evaluation of their antimicrobial activities. International Journal of Physical Sciences, 13: 24-32. http://dx.doi.org/10.5772/intechopen.85698
29. Ravichandran V, Vasanthi S, Shalini S, Shah SAA, Harish R. (2016) Green synthesis of silver nanoparticles using Atrocarpusaltilis leaf extract and the study of their antimicrobial and antioxidant activity. Materials Letters 180: 264-267.https://doi.org/10.1016/j.matlet.2016.05.172
30. Sudha A, Jeyakanthan J, and Srinivasan P (2017) Green synthesis of silver nanoparticles using Lippianodiflora aerial extract and evaluation of their antioxidant, antibacterial and cytotoxic effects. Resource-Efficient Technologies 3: 506-515.https://doi.org/10.1016/j.reffit.2017.07.002
31. Edison TNJI, Lee YR, Sethuraman MG (2016) Green synthesis of silver nanoparticles using Terminalia cuneata and its catalytic action in reduction of direct yellow-12 dye. SpectrochimicaActa Part A: Molecular and Biomolecular Spectroscopy 161: 122-129. https://doi.org/10.1016/j.saa.2016.02.044
32. Rajesh KM, Ajitha B, Reddy YAK, Suneetha Y, Reddy PS (2018) Assisted green synthesis of copper nanoparticles using Syzygium aromaticum bud extract: Physical, optical, and antimicrobial properties. Optik 154: 593-600. https://doi.org/10.1016/j.ijleo.2017.10.074
33. Ismail M, Khan MI, Khan SB, Khan MA, Akhtar K, Asiri AM (2018) Green synthesis of plant-supported CuAg and CuNi bimetallic nanoparticles in the reduction of nitrophenols and organic dyes for water treatment. Journal of Molecular Liquids 260: 78-91. https://doi.org/10.1016/j.molliq.2018.03.058
34. Awwad AM, Salem NM, Abdeen AO (2013) Green synthesis of silver nanoparticles using carob leaf extract and its antibacterial activity. International journal of Industrial chemistry 4: 29-34. https://doi.org/10.1186/2228-5547-4-29
35. Ahmed S, Saifullah Ahmad M, Swami BL, Ikram S (2016) Green synthesis of silver nanoparticles using Azadirachta indica aqueous leaf extract. Journal of radiation research and applied sciences 9:

1-7. https://doi.org/10.1002/mds3.10158

36. Gopinath K, Kumaraguru S, Bhakyaraj K, Mohan S, Venkatesh KS, Esakkirajan M, Kaleeswarran P, Alharbi NS, Kadaikunnan S, Govindarajan M, Benelli G (2016) Green synthesis of silver, gold and silver/gold bimetallic nanoparticles using the Gloriosa superba leaf extract and their antibacterial and antibiofilm activities. Microbial pathogenesis 101: 1-11. https://doi.org/10.1016/j.micpath.2016.10.011
37. Mamatha G, VaradaRajulu A, Madhukar K (2018) In situ generation of bimetallic nanoparticles in cotton fabric using aloe vera leaf extract as a reducing agent. Journal of Natural Fibers 130: 1-9. https://doi.org/10.1080/15440478.2018.1558146
38. Sadanand V, Rajini N, Rajulu AV, Satya narayana B (2016) Preparation of cellulose composites with in situ generated copper nanoparticles using leaf extract and their properties. Carbohydrate polymers 150: 3239. https://doi.org/10.1016/j.carbpol.2016.04.121
39. Sharma G, Kumar A, Naushad M, Kumar A, Ala'a H, Dhiman P, Ghfar AA, Stadler FJ, Khan MR (2018) Phytoremediation of toxic dye from the aqueous environment using monometallic and bimetallic quantum dots-based nanocomposites. Journal of cleaner production 172: 2919-2930. https://doi.org/10.1016/j.jclepro.2017.11.122
40. Crespo P, Litrán R, Rojas TC, Multigner M, De la Fuente JM, Sánchez-López, JC, García MA, Hernando A, Penadés S, Fernández A (2004) Permanent magnetism, magnetic anisotropy, and hysteresis of thiol-capped gold nanoparticles. Physical review letters 93: 872-883. https://doi.org/10.1103/PhysRevLett.93.087204
41. Wang L, Luo J, Shan S, Crew E, Yin J, Zhong CJ, Wallek B, Wong SS (2011) Bacterial inactivation using silver-coated magnetic nanoparticles as functional antimicrobial agents. Analytical chemistry 83: 8688-8695. https://doi.org/10.1021/ac202164p
42. Burdușel AC, Gherasim O, Grumezescu AM, Mogoantă L, Ficai A, Andronescu E (2018) Biomedical applications of silver nanoparticles: an up-to-date overview. *Nanomaterials 8*: 681-690**.** https://doi.org/10.3390/nano8090681
43. Mallakpour, S., Hussain, C.M., Gulati, S., Kumar, S., Diwan, A., Singh, P. and Mongia, A., 2021. “Nanosilver”: A Versatile and New-Generation Nanoproduct in Biomedical Applications. *Handbook of Consumer Nanoproducts*, pp.1-20. https://doi.org/10.1007/978-981-15-6453-6_48-1
44. Sathiyanarayanan, G., Dineshkumar, K. and Yang, Y.H., 2017. Microbial exopolysaccharide-mediated synthesis and stabilization of metal nanoparticles. *Critical reviews in microbiology*, *43*(6), pp.731-752. https://doi.org/10.1080/1040841X.2017.1306689
45. Setyawati, M.I., Yuan, X., Xie, J. and Leong, D.T., 2014. The influence of lysosomal stability of silver nanomaterials on their toxicity to human cells. *Biomaterials*, *35*(25), pp.6707-6715. https://doi.org/10.1016/j.biomaterials.2014.05.007
46. Ajdary, M., Moosavi, M.A., Rahmati, M., Falahati, M., Mahboubi, M., Mandegary, A., Jangjoo, S., Mohammadinejad, R. and Varma, R.S., 2018. Health concerns of various nanoparticles: A review of their in vitro and in vivo toxicity. *Nanomaterials*, *8*(9), p.634. https://doi.org/10.3390/nano8090634

47. Yelton, A.P., Comolli, L.R., Justice, N.B., Castelle, C., Denef, V.J., Thomas, B.C. and Banfield, J.F., 2013. Comparative genomics in acid mine drainage biofilm communities reveals metabolic and structural differentiation of co-occurring archaea. *BMC genomics*, *14*(1), pp.1-15. https://doi.org/10.1186/1471-2164-14-485
48. Lee, H.J., Lee, G., Jang, N.R., Yun, J.H., Song, J.Y. and Kim, B.S., 2011. Biological synthesis of copper nanoparticles using plant extract. *Nanotechnology*, *1*(1), pp.371-374.
49. Murthy, H.C., Desalegn, T., Kassa, M., Abebe, B. and Assefa, T., 2020. Synthesis of green copper nanoparticles using medicinal plant hagenia abyssinica (Brace) JF. Gmel. leaf extract: Antimicrobial properties. *Journal of Nanomaterials*, *2020*. https://doi.org/10.1155/2020/3924081
50. Anand, U., Jacobo-Herrera, N., Altemimi, A. and Lakhssassi, N., 2019. A comprehensive review on medicinal plants as antimicrobial therapeutics: potential avenues of biocompatible drug discovery. *Metabolites*, *9*(11), p.258. https://doi.org/10.3390/metabo9110258
51. Mureed, S., Naz, S., Haider, A., Raza, A., Ul-Hamid, A., Haider, J., Ikram, M., Ghaffar, R., Irshad, M., Ghaffar, A. and Saeed, A., 2021. Development of multi-concentration Cu: Ag Bimetallic nanoparticles as a promising bactericidal for antibiotic-resistant bacteria as evaluated with molecular docking study. *Nanoscale Research Letters*, *16*(1), pp.1-12. https://doi.org/10.1186/s11671-021-03547-6
52. Doolotkeldieva, T., Bobusheva, S., Zhasnakunov, Z. and Satybaldiev, A., 2022. Biological Activity of Ag and Cu Monometallic Nanoparticles and Ag-Cu Bimetallic Nanocomposites against Plant Pathogens and Seeds. *Journal of Nanomaterials*, *2022*. https://doi.org/10.1155/2022/1190280

Figures

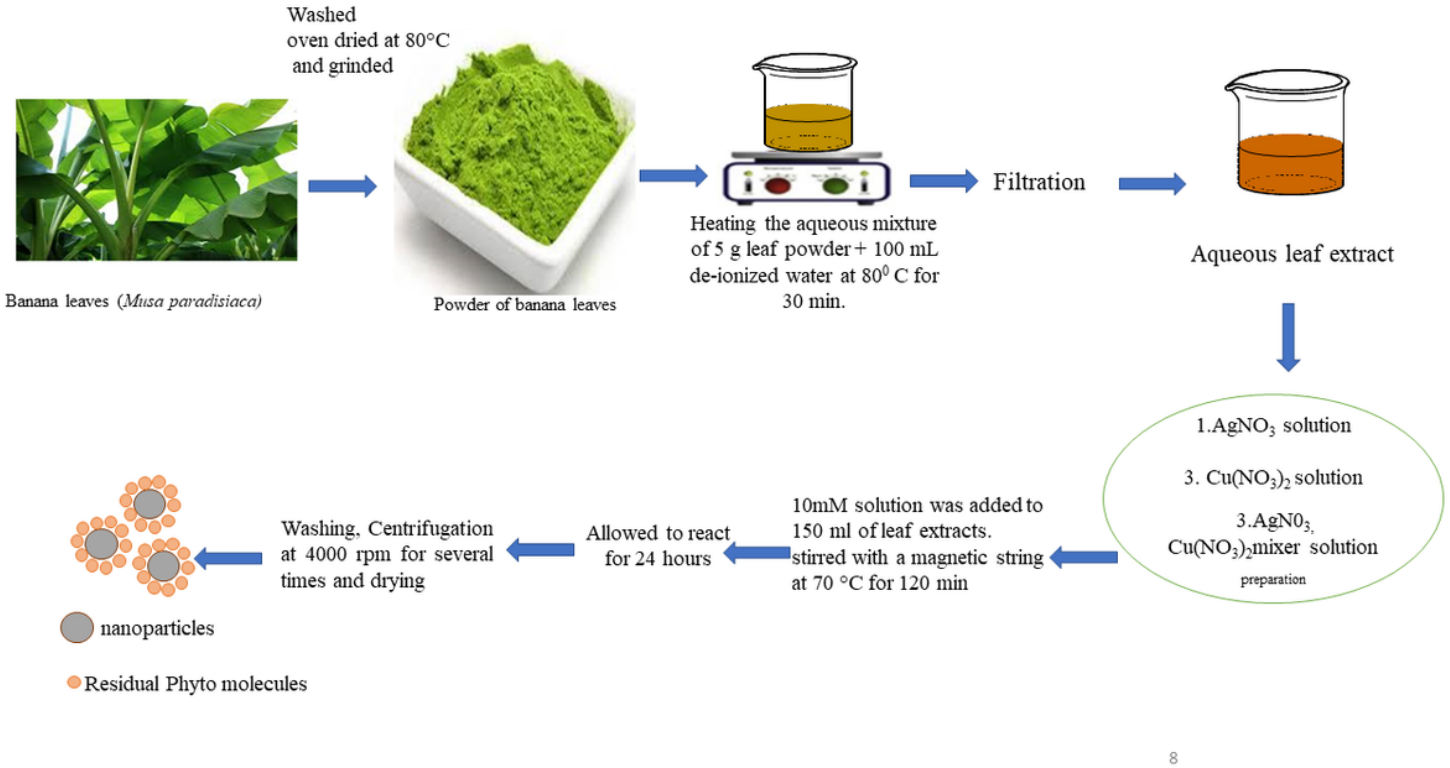

Figure 1

Systematic flowchart of Cu NPs, Ag NPs, and Cu-Ag bimetallic nanoparticles

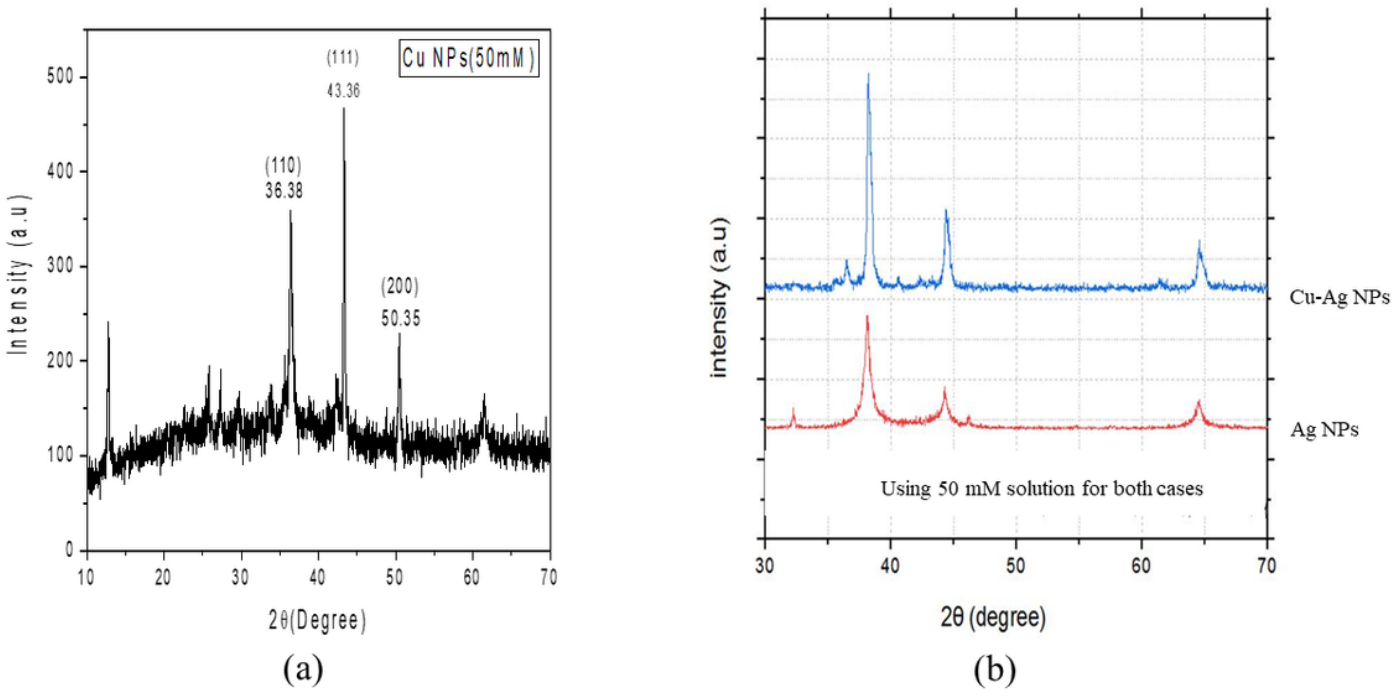

Figure 2

(a) XRD patterns of the green synthesized (By Banana leaf extract) Cu NPs (b) XRD patterns of the green synthesized (By Banana leaf extract) Ag NPs and Cu-Ag NPS

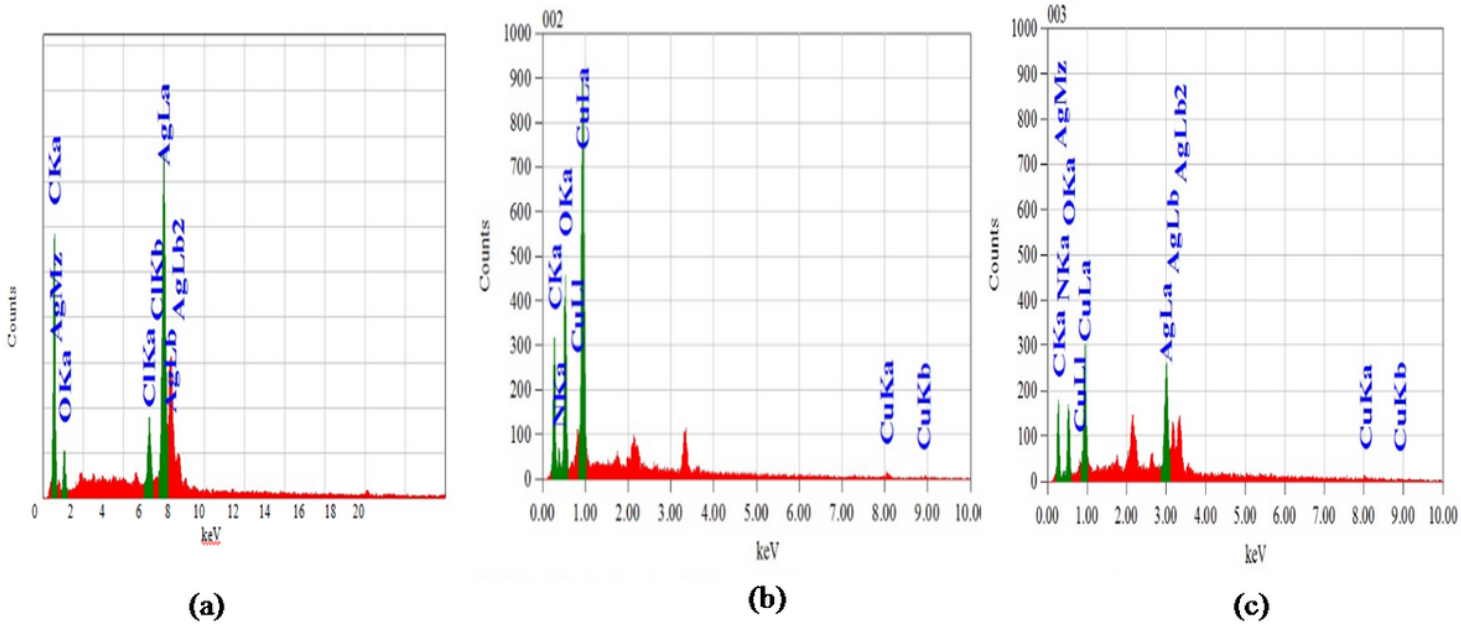

Figure 3

EDS image showing the presence of (a)Cu NPs, (b) Ag NPsand (c) Cu Ag NPs bio-organic components coming from *Musa paradisiaca* leaf extract.

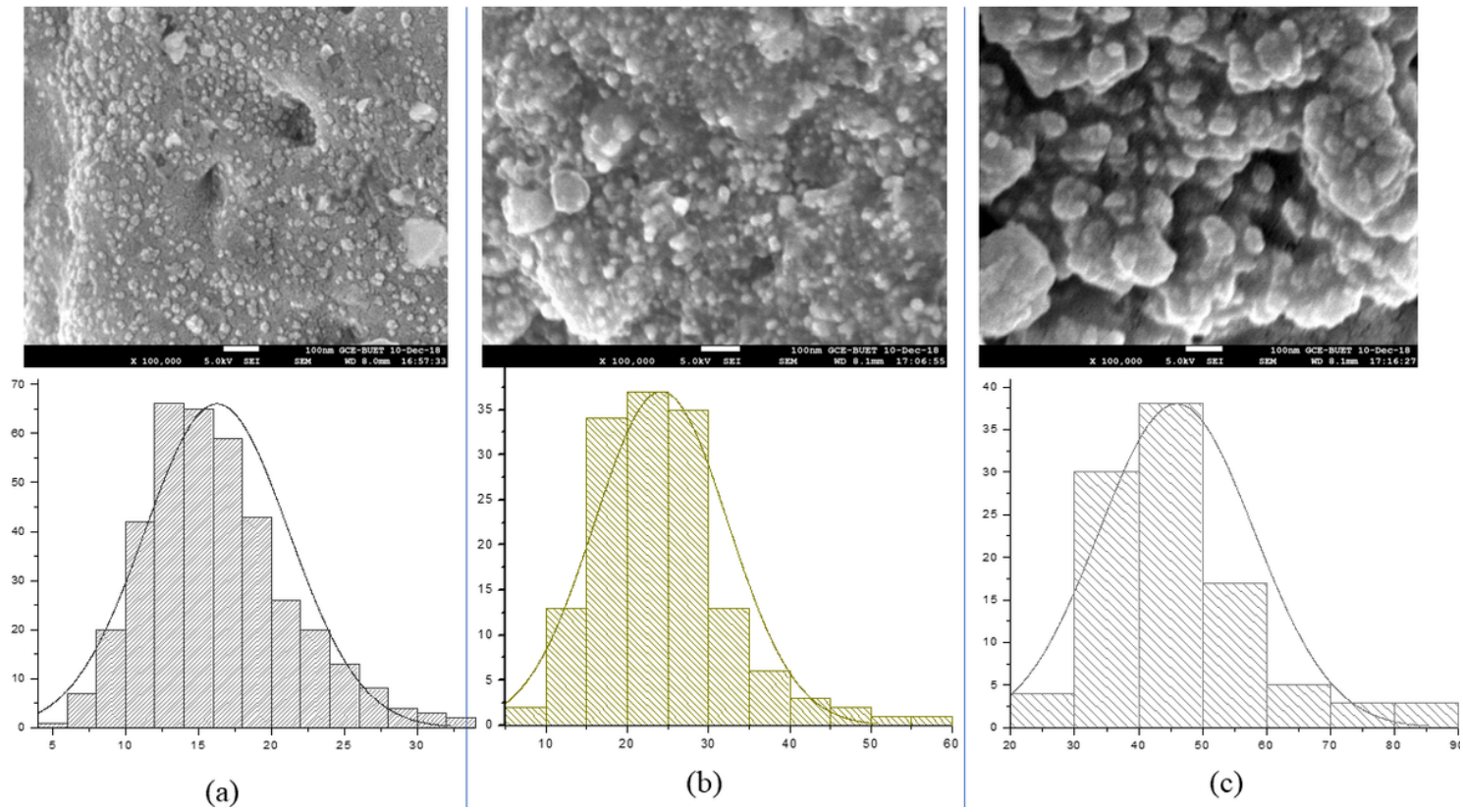

Figure 4

FESEM micrographs and distribution curves of the biosynthesized (a)Cu NPs, (b)Ag NPs, and (c)Cu Ag NP

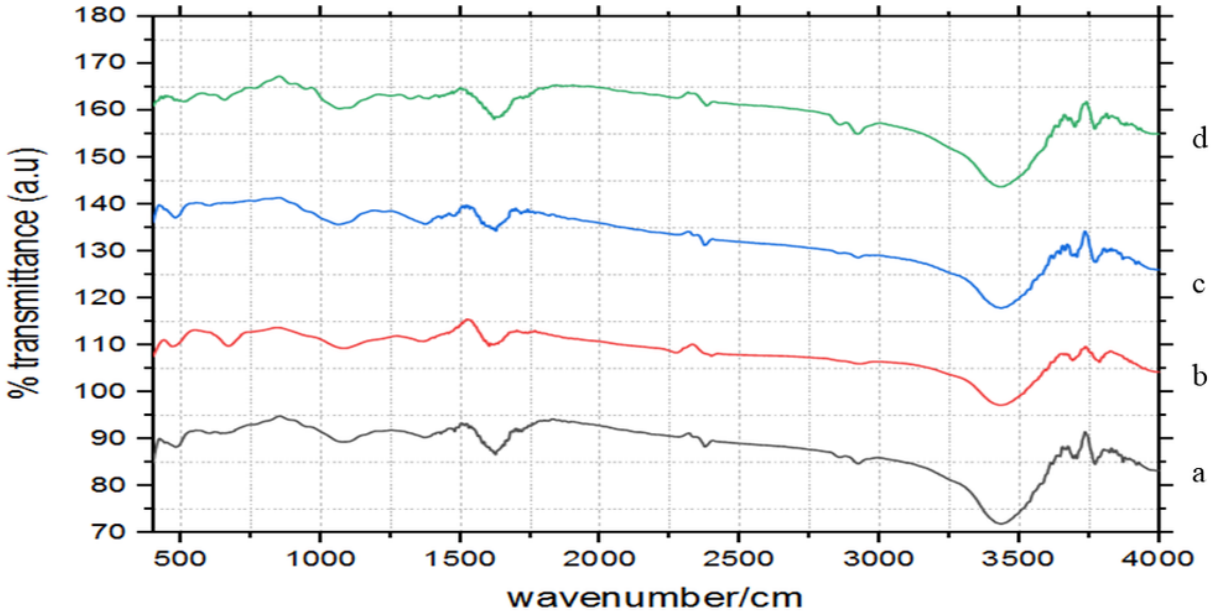

Figure 5

(FT-IR) spectra analysis of Banana leaf, Banana leaf extract mediated (a) Cu NPs, (b) Ag NPs, (c) Cu-Ag NPs, and (d) *Musa paradisiaca* **leaf (Banana leaf) powder.**

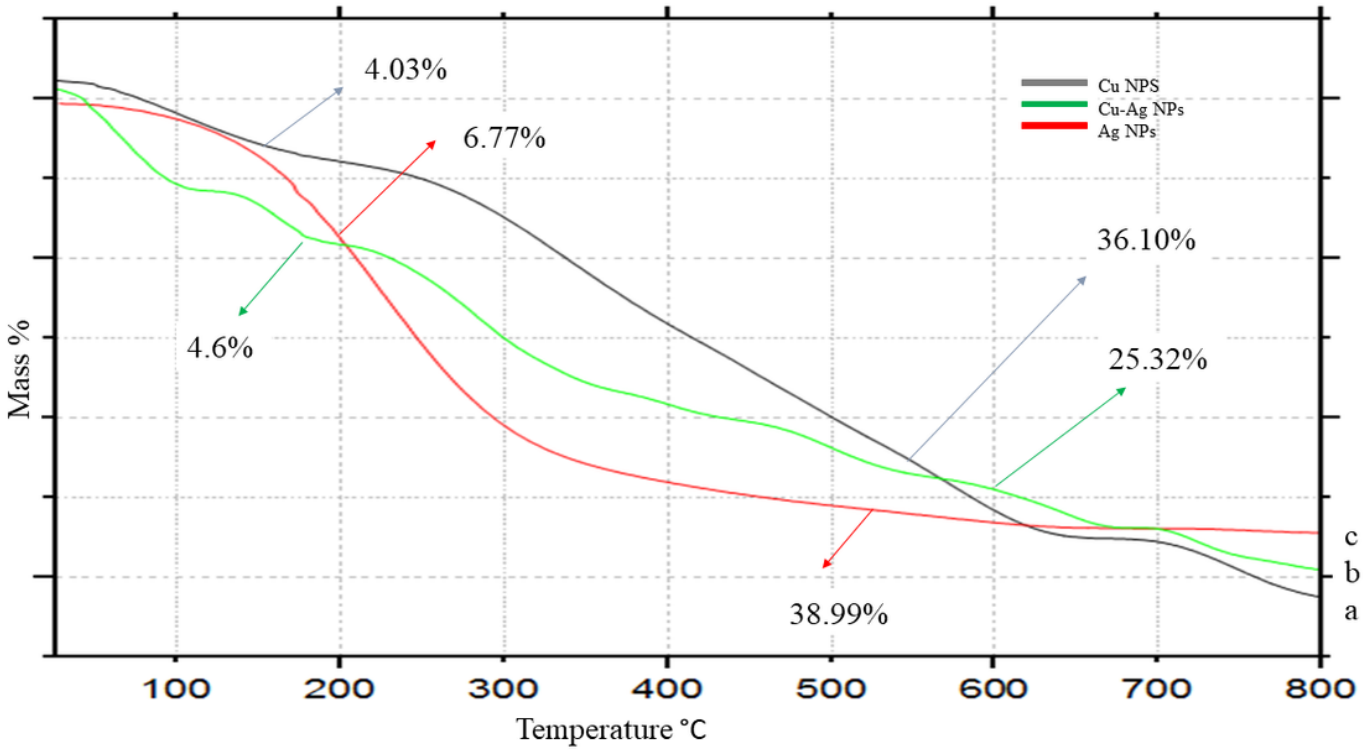

Figure 6

Thermogravimetric Analysis (TGA) of (a) Cu NPs, (b) Cu-Ag NPs, and (c) Ag NPs

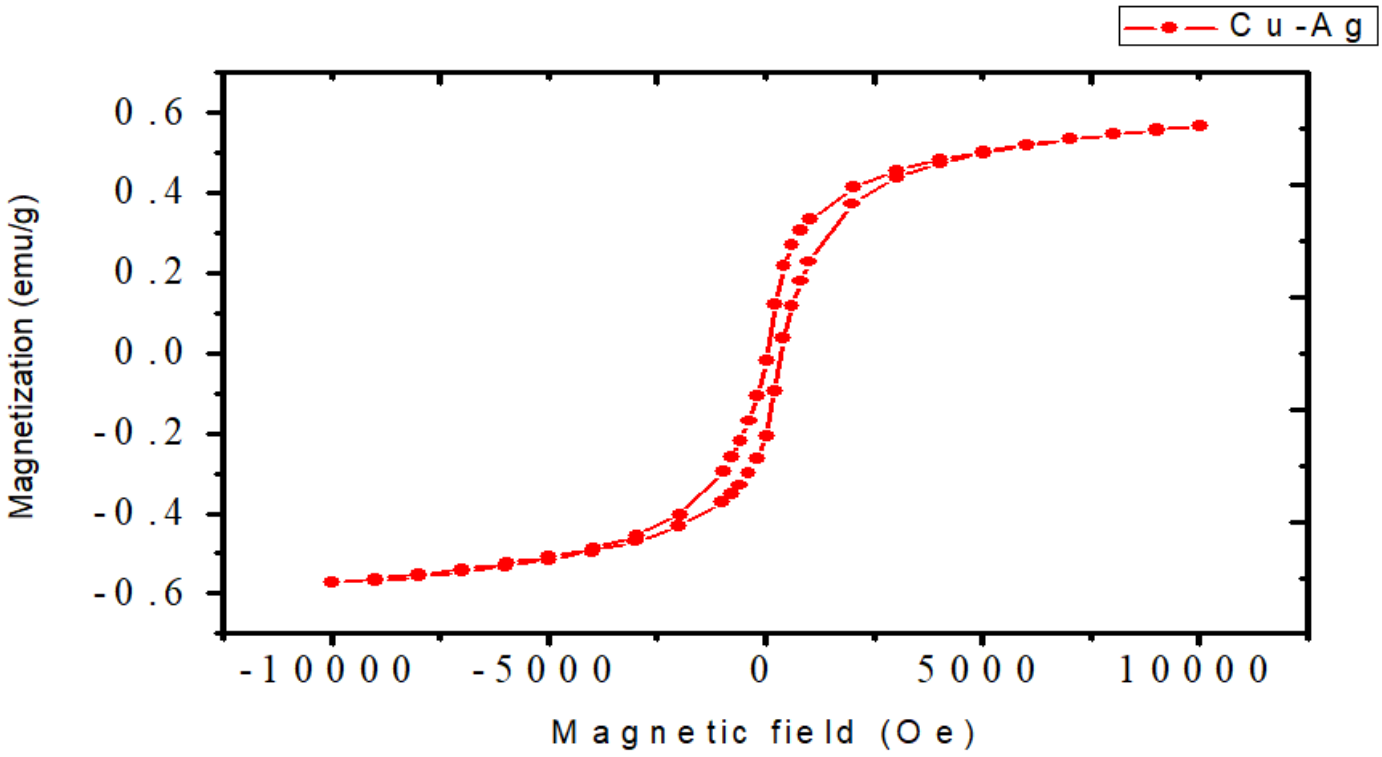

Figure 7

Magnetization curve of synthesized Cu-Ag nanoparticles synthesized using *Musa paradisiaca* leaf (banana leaf) extract